Stability Comparison of New Simplified Speed Sensorless Vector Control Systems for Induction Motors

Glanny M. Ch. Mangindaan[*], Mineo Tsuji[**] and Sin-ichi Hamasaki[***]

Abstract – This paper discusses stability of new simplified sensorless vector control systems of induction motors (IM). The simplified sensorless systems estimate the flux angle by using the output voltage of d-axis PI current controller to achieve the q-axis flux zero. Two simplified sensorless systems are studied. The difference of two systems is the presence or absence of a q-axis PI current controller. The systems stability is compared by deriving linear state equations and showing root loci and unstable regions. Furthermore, transient responses and experiment results make clear the stability of the proposed system.

Keywords: Speed sensorless vector control, Induction motor, D-axis voltage, Root loci, Stability

1. Introduction

A considerable amount of papers have been published in order to improve the performance of an induction motor control without speed sensor, and some of its publications are in [1] - [6]. However, the disadvantage of these systems is complexity. For example, a model reference adaptive system (MRAS) based methods need a state observer and many PI controllers (d-q currents, speed and speed estimation). Furthermore, the systems may become unstable at low speed regenerating operations.

On the other hand, we have proposed a simplified sensorless vector control method of IM in the previous research [7] (we call system A). In this paper, we study the system B in which the q-axis PI current controller is contained and we discuss the stability of systems A and B. A linear model of the system B is derived in state space equation by taking a small perturbation. Stability analysis is performed by showing root loci of the linear models. By the stability analysis, we can determine the gains of controller. From the results of root loci, the unstable region of regenerating operation is improved in both systems. The experimental results of system A is shown to clarify the stability analysis and to demonstrate the effectiveness.

2. Proposed Systems

In order to simplify the controller and to stabilize the

*.   Graduate School of Engineering, Nagasaki University, Japan.
     (bb52212201@cc.nagasaki-u.ac.jp)
**. Graduate School of Engineering, Nagasaki University, Japan.
     (mineo@nagasaki-u.ac.jp)
***. Graduate School of Engineering, Nagasaki University, Japan.
     (hama-s@nagasaki-u.ac.jp)

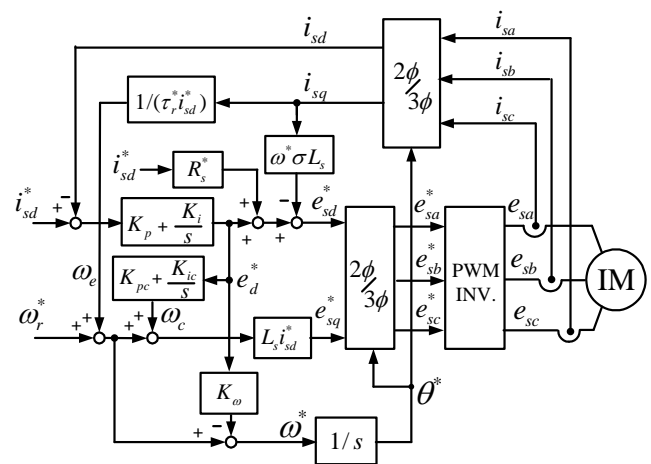system at low speed regenerating operations, we proposed a sensorless vector control system shown in Fig. 1. [7].
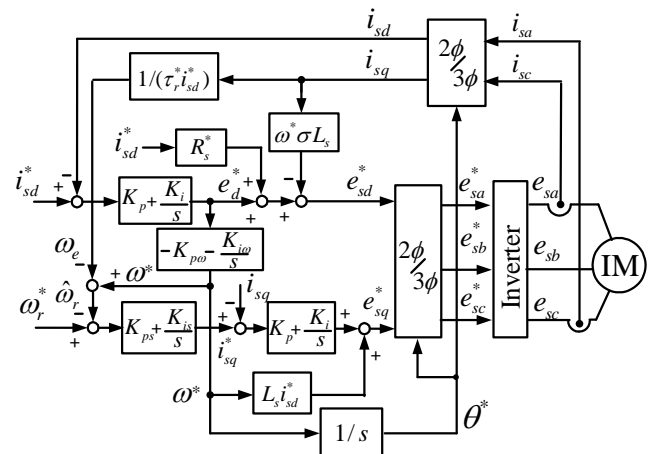

Fig. 1. Block diagram of system A.

Fig. 2. Block diagram of system B.

In this paper, we propose and analyze the system B in which the rotor speed is estimated explicitly and the q-axis PI current controller is contained as shown in Fig. 2.

By neglecting the derivative of d-axis current and flux, the following d-axis voltage model equation is obtained in rotating reference frame [7].

$$e_{sd}^* = R_s^* i_{sd}^* - \omega^* \sigma L_s i_{sq} - \omega^* M \psi_{rq}^v / L_r \tag{1}$$

By using the e_d^* which is the output of d–axis PI current controller in Fig. 2, we have:

$$e_d^* = -\omega^* M \psi_{rq}^v / L_r \tag{2}$$

We estimate the flux frequency ω^* to bring q–axis flux ψ_{rq}^v to zero by using PI controller as

$$\omega^* = -\left(K_{p\omega} + \frac{K_{i\omega}}{s} \right) e_d^* \tag{3}$$

where,

$$K_{p\omega} = \text{sign}\left(\omega^*\right)\left|K_{p\omega}\right| \text{ and } K_{i\omega} = \text{sign}\left(\omega^*\right)\left|K_{i\omega}\right|$$

The estimated speed $\hat{\omega}_r$ is computed by using slip speed ω_e. In Fig. 2, the PI speed controller and the PI current controllers are composed as conventional system. Flux angle θ^* is obtained by integrating ω^* as:

$$\theta^* = \omega^* / s \tag{4}$$

3. Analytical Model

In the previous paper, we analyzed the system A [7]. Therefore, we analyze the system B in this paper. By using the d–q model of IM which rotates synchronously with θ^* and the equations of controller, a non-linear state equation of the system B is obtained as

$$p\mathbf{x} = \mathbf{f}\left(\mathbf{x}, i_{sd}^*, \omega_r^*, T_L\right) \tag{5}$$

where,

$$\mathbf{x} = \begin{bmatrix} i_{sd} & i_{sq} & \psi_{rd} & \psi_{rq} & \omega_r & e_{cd} & e_\omega & \omega_{cd} & e_{cq} \end{bmatrix}^T \tag{6}$$

The state variables e_{cd} and e_{cq} are necessary for PI current controllers, and e_ω and ω_{cd} are necessary for PI flux speed estimator and PI speed controller respectively. The transient responses are computed by solving (5).

We derive a linear model to study the stability of system B by considering small perturbation about a steady-state operating point:

$$p\Delta\mathbf{x} = \mathbf{A}\Delta\mathbf{x} + \mathbf{B}\Delta\omega_r^* + \mathbf{B}_L\Delta T_L \tag{7}$$

where:

$$\Delta\mathbf{x} = \begin{bmatrix} \Delta i_{sd}, \Delta i_{sq}, \Delta\psi_{rd}, \Delta\psi_{rq}, \Delta\omega_r, \Delta e_{cd}, \Delta e_\omega, \Delta\omega_{cd}, \Delta e_{cq} \end{bmatrix}^T$$

$$a_1 = \frac{R_s}{\sigma L_s} + \frac{M^2}{\sigma L_s L_r \tau_r} + \frac{K_p}{\sigma L_s}, \quad a_2 = \frac{M P^2}{4 J L_r},$$

$$a_3 = \frac{K_p K_{ps} - L_s^* i_{sd}^*}{\sigma L_s} + i_{sd}, \quad a_4 = \frac{M}{\sigma L_s L_r \tau_r}$$
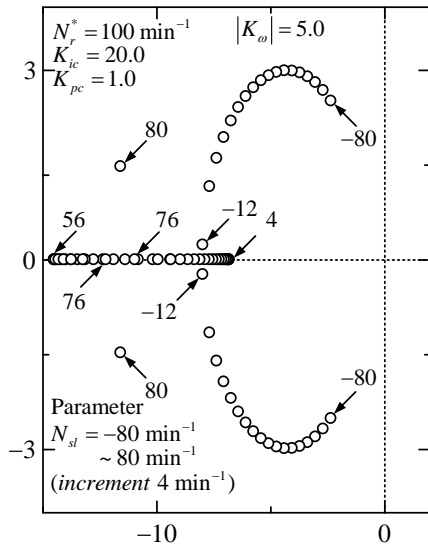
$$\mathbf{A} = \begin{bmatrix} -a_1 & 0 & a_4 & \dfrac{M\omega_r}{\sigma L_s L_r} \\[2ex] -\omega^* - K_p K_{p\omega} a_3 & -a_1 + \dfrac{K_p K_{ps}}{\sigma L_s \tau_r^* i_{sd}^*} & -\dfrac{M\omega_r}{\sigma L_s L_r} & a_4 \\[2ex] \dfrac{M}{\tau_r} + K_p K_{p\omega} \psi_{rq} & 0 & -\dfrac{1}{\tau_r} & \omega^* - \omega_r \\[2ex] -K_p K_{p\omega}\psi_{rd} & \dfrac{1}{\tau_r}M & \omega_r - \omega^* & -\dfrac{1}{\tau_r} \\[1.5ex] -a_2\psi_{rq} & a_2\psi_{rd} & a_2 i_{sq} & -a_2 i_{sd} \\[1ex] -K_i & 0 & 0 & 0 \\[1ex] K_{i\omega}K_p & 0 & 0 & 0 \\[1.5ex] -K_{is}K_{p\omega}K_p & \dfrac{K_{is}}{\tau_r^* i_{sd}^*} & 0 & 0 \\[2ex] K_i K_{ps}K_{p\omega}K_p & K_i\left(\dfrac{K_{ps}}{\tau_r^* i_{sd}^*} - 1\right) & 0 & 0 \end{bmatrix} *$$

$$* \begin{bmatrix} \dfrac{M\psi_{rq}}{\sigma L_s L_r} & \dfrac{1}{\sigma L_s} & 0 & 0 & 0 \\[2ex] -\dfrac{M\psi_{rd}}{\sigma L_s L_r} & K_{p\omega}a_3 & -a_3 & \dfrac{K_p}{\sigma L_s} & \dfrac{1}{\sigma L_s} \\[1.5ex] -\psi_{rq} & -K_{p\omega}\psi_{rq} & \psi_{rq} & 0 & 0 \\[1ex] \psi_{rd} & K_{p\omega}\psi_{rd} & -\psi_{rd} & 0 & 0 \\[1ex] 0 & 0 & 0 & 0 & 0 \\[1ex] 0 & 0 & 0 & 0 & 0 \\[1ex] 0 & -K_{i\omega} & 0 & 0 & 0 \\[1ex] 0 & K_{is}K_{p\omega} & -K_{is} & 0 & 0 \\[1ex] 0 & K_i K_{ps}K_{p\omega} & -K_i K_{ps} & K_i & 0 \end{bmatrix}$$
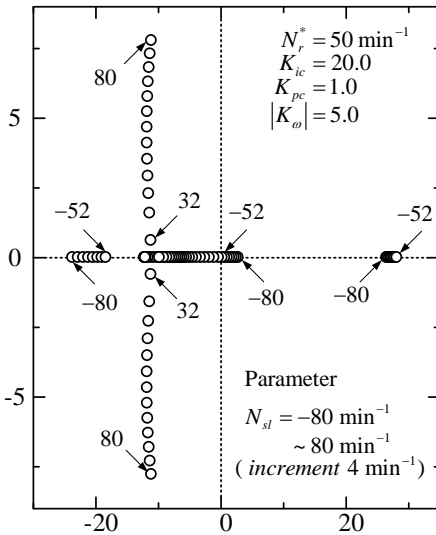
$$\mathbf{B} = \begin{bmatrix} 0 \\ \dfrac{K_p K_{ps}}{\sigma L_s} \\ 0 \\ 0 \\ 0 \\ 0 \\ 0 \\ K_{is} \\ K_i K_{ps} \end{bmatrix} ; \quad \mathbf{B}_L = \begin{bmatrix} 0 \\ 0 \\ 0 \\ 0 \\ -\dfrac{P}{2J} \\ 0 \\ 0 \\ 0 \\ 0 \end{bmatrix}$$

We confirmed that the transient responses of the linear model are in good agreement with those of the nonlinear model around the steady state operating point. The linear model can not analyze the discrete points caused by the limiters.

4. Transient Characteristics

at low speed regenerating operation. However, the system is unstable at plugging region as shown in (b) by the poles on real axis in both systems.

(a) $N_r^* = 100$ min^{-1}

(b) $N_r^* = 50$ min^{-1}

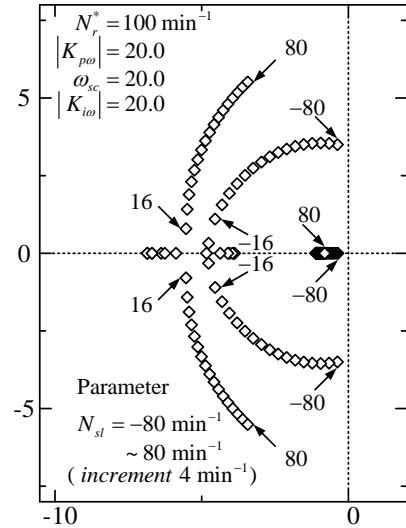**Fig. 3.** Trajectories of poles (system A).

(a) $N_r^* = 100$ min^{-1}
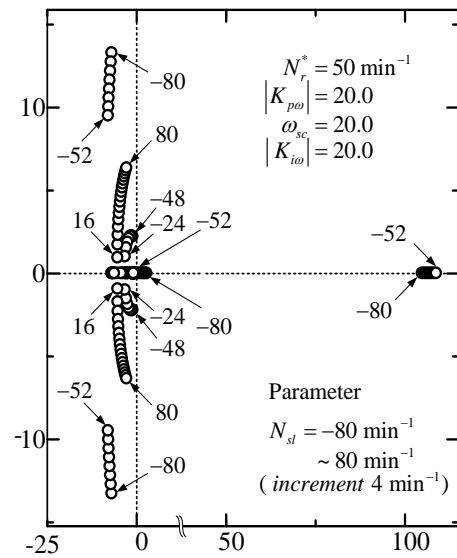
(b) $N_r^* = 50$ min^{-1}

Fig. 4. Trajectories of poles (system B).

The proposed control system is implemented by a DSP (TMS320C32)-based PWM inverter. A compensating method is developed for the experimental system for dead time and the non-ideal features of IGBT [8]. Parameters of IM are: number of pole P=4, stator resistance R_s =1.54Ω, rotor resistance R_r=0.787Ω, stator and rotor inductance L_s=L_r=0.115H, mutual inductance M=0.11H, and moment of inertia J=0.0126 kgm^2.

Figs. 3 and 4 show the root trajectories computed by the linear models of systems A and B respectively. The speed command N_r^* is 100 min^{-1} in case (a), 50 min^{-1} in case (b) and slip speed N_{sl} is changed from –80 min^{-1} to 80 min^{-1} (T_L =9.07Nm) as a parameter of load. The system is stable

Fig. 5 shows the unstable operating region when speed command and slip speed are changed with parameters $|K_\omega|$ = 5.0 , K_{ic} = 20.0 and K_{pc} = 1.0 for system A. In earlier paper, we have only studied when K_{pc} = 0.0 [9]. The increasing value of speed control proportional gain K_{pc} can improve the stability region at low speed of motoring and plugging operations [7]. Fig. 6 shows the unstable operating region of system B with parameters; $|K_{p\omega}|$ =20.0, $|K_{i\omega}|$ =20.0, and ω_{sc} =20.0. The ω_{sc} is the cut-off angular frequency of the speed control. These gains are selected to have wide stable operating points. By comparing the results of Figs. 5 and 6, it is found that unstable plugging region is almost same.

Fig. 7 shows the transient responses of the system B computed by non-linear model (5). The speed command is changed from 50min^{-1} to 150min^{-1} and then to 50min^{-1} when the system is operated at regenerating operation.
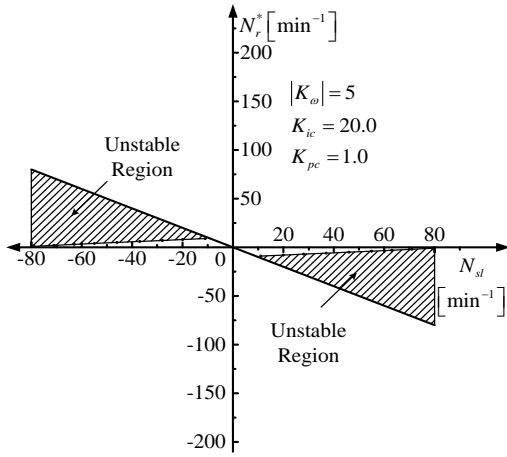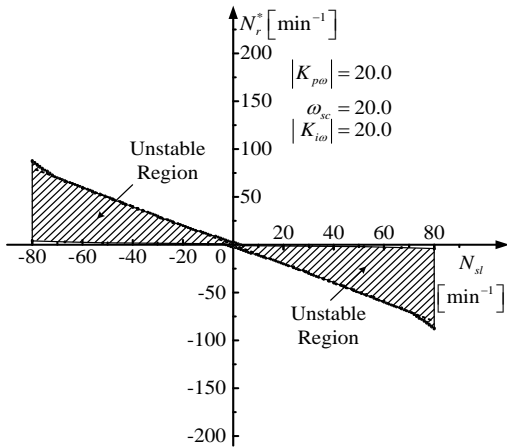

Fig.5. Unstable regions of system A.

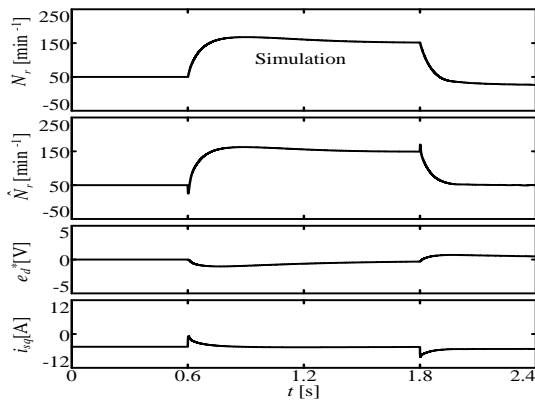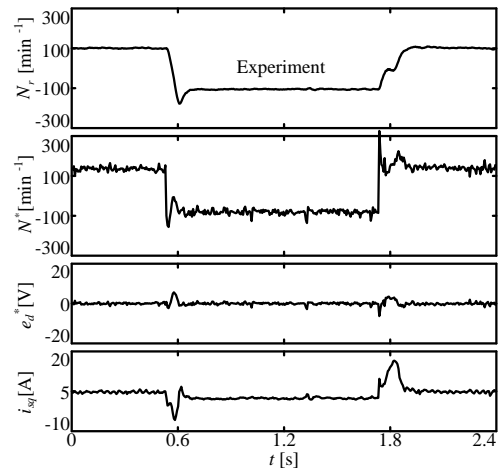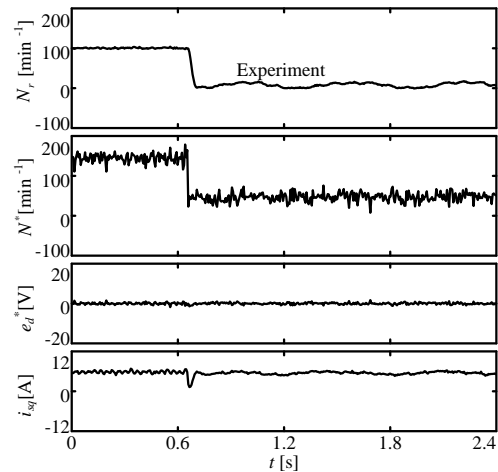**Fig. 6.** Unstable regions of system B.

$(50 \rightarrow 150 \rightarrow 50 \text{ min}^{-1}, \quad K_{p\omega} = 20.0, \omega_{sc} = 20.0, \text{ and } K_{i\omega} = 20.0)$

Fig. 7. Transient responses of system B at $T_L = -4.0$ N-m.

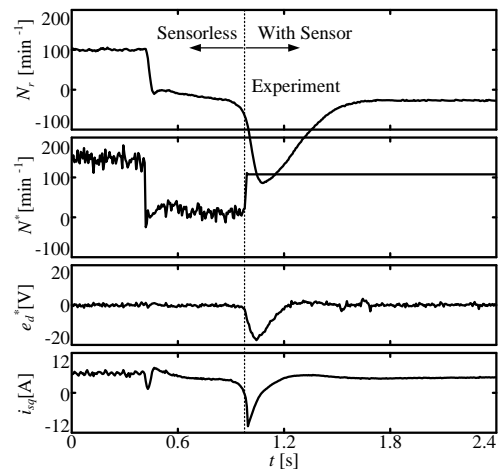$(100 \rightarrow -100 \rightarrow 100 \text{ min}^{-1}, \quad |K_\omega| = 5.0, K_{ic} = 20.0, K_{pc} = 1.0)$

(a) Load torque $T_L = 4.0$ N-m

$(100 \rightarrow 5.0 \text{ min}^{-1}, \quad |K_\omega| = 5.0, K_{ic} = 20.0, K_{pc} = 1.0)$
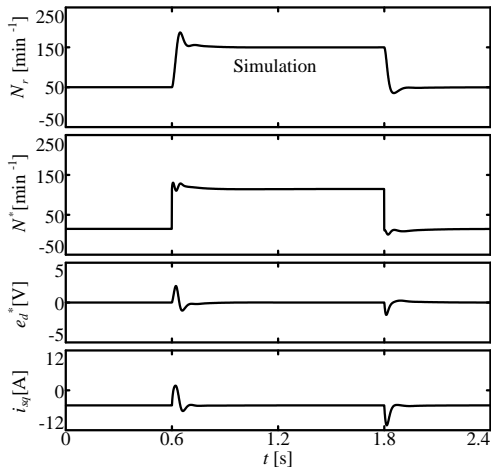
(b) Load torque $T_L = 5.0$ N-m

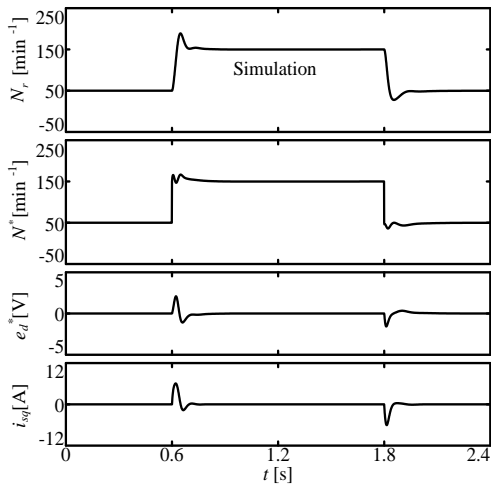$(100 \rightarrow -25.0 \text{ min}^{-1}, \quad |K_\omega| = 5.0, K_{ic} = 20.0, K_{pc} = 1.0)$
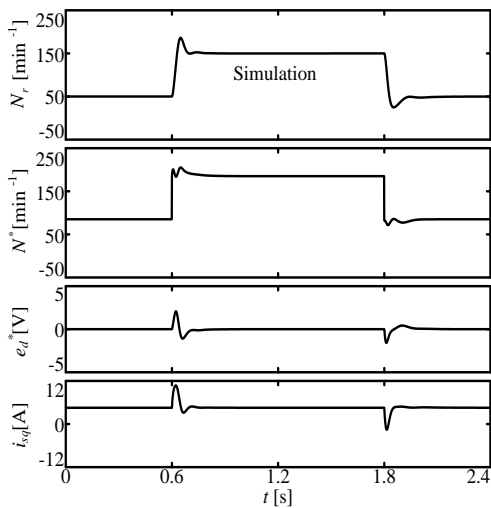
(c) Load torque $T_L = 5.0$ N-m

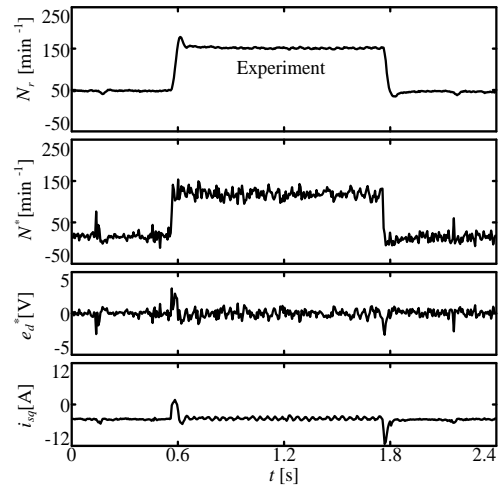**Fig. 8.** Transient responses of system A.

(a) Load torque T_L =-4.0 N-m

(a) Load torque T_L =-4.0 N-m

(b) Load torque T_L =0.0 N-m

(b) Load torque T_L =0.0 N-m

(c) Load torque T_L =4.0 N-m

$(50 \rightarrow 150 \rightarrow 50$ min^{-1}, $|K_\omega|$ =5.0, K_{ic} =20.0, K_{pc} =1.0)

Fig. 9. Transient responses of system A.
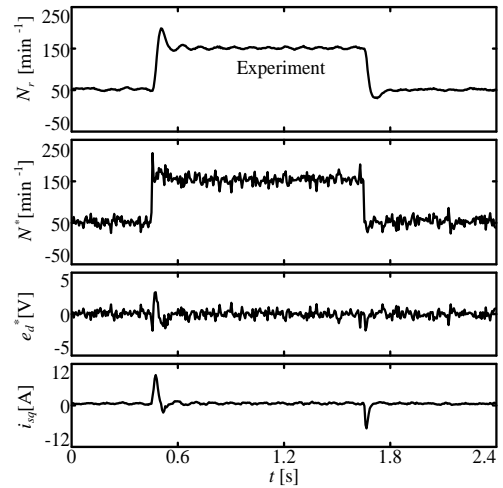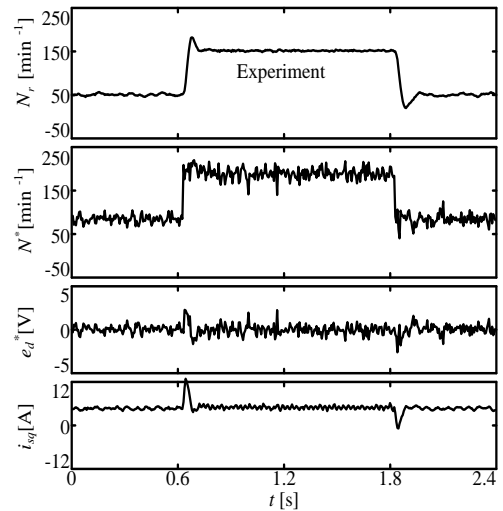

(c) Load torque T_L =4.0 N-m

$(50 \rightarrow 150 \rightarrow 50$ min^{-1}, $|K_\omega|$ =5.0, K_{ic} =20.0, K_{pc} =1.0)

Fig. 10. Transient responses of system A.

Fig. 8 shows the experimental results of system A. Fig (a) shows the responses when the speed command is changed from 100min^{-1} to -100min^{-1} and then to 100min^{-1}. N_r is the rotor speed and N^* is the synchronous speed. In Fig. (b), the speed command is changed from 100min^{-1} to 5min^{-1}. In these cases, the system can be operated stably. On the other hand, in Fig.(c), the speed command is changed from 100min^{-1} to -25min^{-1}. The system becomes unstable at plugging region and is operated using speed sensor for the protection after $t = 0.98$s. This experimental result can prove the unstable region of Fig.5.

Fig. 9 shows the simulation results of non-linear model of system A for each parameters of load torque T_L when the speed command is changed from 50 min^{-1} to 150 min^{-1} and then to 50 min^{-1}. The speed responses give almost the same characteristics for each load torque. However, the i_{sq} differs from each parameter of T_L. Fig. 10 shows the experimental results corresponding to the simulation results of Fig. 9. It is confirmed that the experimental results agree well with the theoretical results except for high frequency ripples. The high frequency ripples are caused by PWM voltage control in experimental system.

5. Conclusion

We have discussed the comparison of proposed sensorless vector control systems of IM. The results obtained from this study are summarized as follows:

(1) Flux angle computation and control of torque- speed are constructed by using the output voltage of d-axis PI current controller.

(2) The operation at plugging region which is computed by using a linear model is almost unstable for both systems A and B.

(3) Both systems A and B can realize stable operation in both motoring and regenerating operations.

(4) The experimental results could prove the validity of the theory. Especially instability phenomenon of plugging region is observed experimentally.

(5) Simpler structure of the system A is preferable than the system B from the viewpoints (2) and (3).

References

[1] C. Schauder, "Adaptive speed identification for vector control of induction motors without rotational transducers", *IEEE Trans. Industr. Applic.*, Vol.28, No.5, pp. 1054-1061, Sep./Oct. 1992.

[2] H. Tajima, Y. Hori, "Speed sensorless field orientation control of the induction machine." *IEEE IAS Annual Meeting*, pp. 385-391, 1991.

[3] H. Kubota, K. Matsuse, "Speed sensorless field oriented control of induction machines using flux observer", *IEEE IECON*, pp. 1611-1615, 1994.

[4] H. Sugimoto, L. Ding, "A consideration about stability of vector controlled induction motor systems using adaptive secondary flux observer", *Trans. IEEJapan*, Vol.119-D, No.10, pp.1212-1222, 1999.

[5] M. Tursini, R. Petrella, and F. Parasiliti, "Adaptive sliding mode observer for speed sensorless control of induction motors", *IEEE Trans. Industr. Applic.*, Vol.36, No.5, pp.1380-1387, Sep./Oct. 2000.

[6] Y. Kinpara, M. Koyama, "Speed sensorless vector control method of induction motor including a low speed region", *Trans. IEEJapan*, Vol.120-D, No.2, pp.223-229, 2000.

[7] G. M. C. Mangindaan, M. Tsuji, S. Hamasaki, "Transient characteristics of a new simplified speed sensorless vector control for induction motors", *Proc. of International Conference on Electrical Machines and Systems* (ICEMS), pp.2018-2023, 2013.

[8] M. Tsuji, S. Chen, K. Izumi and E. Yamada, "A sensorless vector control system for induction motors using q-axis flux with stator resistance identification", *IEEE Trans. Industrial Electronics*, Vol.48, No.1, pp. 185-194, February 2001.

[9] M. Tsuji, G. M. C. Mangindaan, Y. Kunizaki, S. Hamasaki, "Simplified speed-sensorless vector control for induction motors and stability analysis", *IEEJ Journal of Ind. Appl.*,vol.3 No.2 pp.138 – 145, March 2014.

Glanny M Ch Mangindaan was born in March 1974. He received the B.Eng degree from Sam Ratulangi University and M.Eng degree from Sepuluh Nopember Institute of Technology. He became a lecturer in Division of Electrical Engineering at Sam Ratulangi University in 2002. He has entered as Ph.D. course in Nagasaki University Graduate School of Engineering in 2012. His research interest is about the speed sensorless vector control of AC motors.

Mineo Tsuji was born in December 1953. He received the Ph.D. degree from Kyushu University in March 1981 in electrical engineering, became a Professor at Nagasaki University in July 2001. His current interests are control of AC machines and power systems. He received a Prize Paper Award from the IEEJ in 1998.

Shin-ichi Hamasaki was born in October, 1975. He received the B.E. and M.E. and Ph.D. degrees in electrical engineering from Yokohama National University in 1998, 2000 and 2003 respectively. From 2003 to 2007, he was a Research Associate in Nagasaki University. Since April 2007, he has been an Assistant Professor in the Division of Electrical Engineering and Computer Science. His current research interests are power conditioning systems and motor drives.